PAPER

Exploring and controlling intrinsic defect formation in SnO$_2$ thin films†

Yoann Porte,[a] Robert Maller,[a] Hendrik Faber,[b] Husam N. AlShareef,[c] Thomas D. Anthopoulos[b] and Martyn A. McLachlan*[a]

By investigating the influence of key growth variables on the measured structural and electrical properties of SnO$_2$ prepared by pulsed laser deposition (PLD) we demonstrate fine control of intrinsic n-type defect formation. Variation of growth temperatures shows oxygen vacancies (V$_O$) as the dominant defect which can be compensated for by thermal oxidation at temperatures >500 °C. As a consequence films with carrier concentrations in the range 10^{16}–10^{19} cm^{-3} can be prepared by adjusting temperature alone. By altering the background oxygen pressure (P_D) we observe a change in the dominant defect – from tin interstitials (Sn$_i$) at low P_D (<50 mTorr) to V$_O$ at higher P_D with similar ranges of carrier concentrations observed. Finally, we demonstrate the importance of controlling the composition target surface used for PLD by exposing a target to >100 000 laser pulses. Here carrier concentrations >1 × 10^{20} cm^{-3} are observed that are associated with high concentrations of Sn$_i$ which cannot be completely compensated for by modifying the growth parameters.

Introduction

Transparent conducting oxides (TCOs) are currently implemented extensively in a wide variety of optoelectronic applications including; flat-panel displays, solar-cells, light-emitting diodes and thin film transistors.[1–4] Whilst the development of n-type TCOs have been thoroughly investigated e.g. indium tin oxide (ITO), aluminium doped zinc oxide (AZO), and indium doped zinc oxide (IZO)[5–7] the progress towards developing p-type analogues is significantly lacking, owing to the challenge of obtaining stable p-type characteristics. SnO$_2$ is an intrinsic n-type semiconductor with a wide direct band gap (3.6 eV), high optical transparency and compatibility with a range of deposition methods. SnO$_2$ is perhaps the material that underpins current n-type TCO technology with fluorine doped tin oxide (FTO), antimony doped tin oxide (ATO) and ITO being the most commonly implemented materials. In its stoichiometric form SnO$_2$ is an insulator,[8] however the presence of intrinsic defects creates charge carriers at concentrations large enough to ensure high conductivity. The exact nature of these defects has been the focus of numerous discussions, e.g. Kılıç and Zunger recently calculated that the low formation energy donor type defects of tin interstitials (Sn$_i$) and oxygen vacancies (V$_O$) explain the

n-type behaviour[9] – specifically Sn$_i$ was identified as the majority defect. This has been questioned by Godinho et al.[8] who calculated V$_O$ to have a lower formation energy than Sn$_i$, which was attributed to the dual valence of tin. As a consequence, the reduction of Sn^{4+} to Sn^{2+} can occur and facilitate the formation of V$_O$. However, Sn$_i$ and V$_O$ are not the only defects responsible for n-type conductivity in SnO$_2$. It has been shown by Kılıç and Zunger[10] and Singh et al.[11] that hydrogen incorporation into interstitial sites and substitution onto oxygen sites can explain the observed behaviour – this is consistent with H-donors being attributed to n-type conductivity in other oxide semiconductor systems e.g. ZnO.[12,13]

Although n-type SnO$_2$ is well understood, investigation of p-type conductivity in SnO$_2$ is still challenging and has been investigated intensely over the past decade. Several reports of p-type SnO$_2$ have been made where extrinsic dopants with a lower valence than Sn^{4+} e.g. Al,[14,15] Ga[16,17] and Zn[18] have been incorporated into the structure. The underlying principle lies on substituting such cations on the Sn site to induce the formation of one (or more) hole(s). Although some examples of p-type conductivity have been reported the achieved electronic properties do not reach those necessary for TCO applications. The efficiency of the p-type doping is limited in SnO$_2$ due to self-compensation effect leading to a charge neutrality limit.[19] Furthermore the high dopant concentration required to overcome the charge compensation, i.e. between 10–20 atomic percent (at%), is significantly greater than that required to achieve good n-type behaviour, e.g. 2 at% for Sb.[20] When considering the possibility of demonstrating good p-type characteristics it is critical to consider controlling defect formation

[a] Department of Materials and Centre for Plastic Electronics, Imperial College London, London SW7 2AZ, UK. E-mail: martyn.mclachlan@imperial.ac.uk

[b] Department of Physics and Centre for Plastic Electronics, Imperial College London, London SW7 2BP, UK

[c] Materials Science and Engineering, King Abdullah University of Science and Technology (KAUST), Thuwal 23955-6900, Saudi Arabia

† Electronic supplementary information (ESI) available. See DOI: 10.1039/c5tc03520a

758 | *J. Mater. Chem. C*, 2016, **4**, 758–765

This journal is © The Royal Society of Chemistry 2016

to avoid any impurities or n-type defects susceptible to disrupt the formation of p-type defects. The majority of existing studies conducted on p-type SnO_2 do not highlight the importance of establishing "p-type compatible" conditions to ensure efficient and effective doping that allow for an understanding of the formation of intrinsic defects responsible for n-type conductivity in SnO_2.

In the current study we focus on the influence of the deposition environment and growth parameters in order to control the intrinsic defects of the SnO_2 system. Our chosen growth technique, pulsed laser deposition (PLD), is particularly suitable for this investigation as it facilitates excellent cation transfer from the target materials, allows deposition under a wide range of oxygen pressures[21] (P_D) (thus control of electrical conductivity), supports high deposition rates and allows excellent control of the film growth parameters.[22] We present our results in three parts, describing first the independent variation of deposition temperature (T_D) and P_D and then where the PLD target is changed through multiple interactions with the laser i.e. growth cycles. The experimentally measured properties of our thin films are discussed with consideration to the numerous theoretical calculations contained in the literature to determine the role of donor type defects in SnO_2.

Results and discussion

For the studies where T_D was varied the P_D was fixed at 100 mTorr we investigated the variation of T_D over the range 300–700 °C. In the case of P_D variation T_D was maintained at 600 °C and P_D changed from 5–300 mTorr (0.67–40 Pa). For the target exposure variation our ceramic target was pre-exposed

to >100 000 laser pulses and films then deposited under the same conditions as those prepared when varying T_D and P_D. A commercial SnO_2 target was used owing to the difficulties of sintering dense (∂ > 95%) targets in-house without the use of additives that may contribute to doping.[23]

Influence of deposition temperature (T_D)

The films grown exhibit mainly the casserite phase (SnO_2) with some evidence of SnO being present, shown by the typical X-ray diffraction (XRD) data in Fig. 1a. At 300 °C the films are amorphous with crystalline films deposited at all other temperatures. The crystalline films exhibit a strong (110) orientation with diffraction from the (101), (200) and (211) planes observed to differing extents consistent with other reports.[24] To quantise the preferential orientation of our films the texture coefficient TC(hkl) was calculated using the eqn (1):[25]

$$TC(hkl) = \frac{I(hkl)/I_0(hkl)}{(1/N)\sum I(hkl)/I_0(hkl)} \tag{1}$$

where TC(hkl) is the texture coefficient of the plane, $I(hkl)$ is the integrated peak area, $I_0(hkl)$ the corresponding standard intensity from the ICDD data (here, 01-077-0452) and N the number of diffraction peaks observed. TC was calculated to show a (200) preferred orientation at 400 and 500 °C, changing to a (110) preferred orientation at ≥600 °C. All calculated TC values are shown in Table S1.† From the XRD data we highlight shifts in the (200) diffraction peak position as temperature is increased, Fig. 1b. The temperature dependant peak shifts observed are related to changes in the a-lattice parameter, calculated using eqn (2), where h, k and l are the Miller indexes of the diffracting planes and d is the lattice spacing between
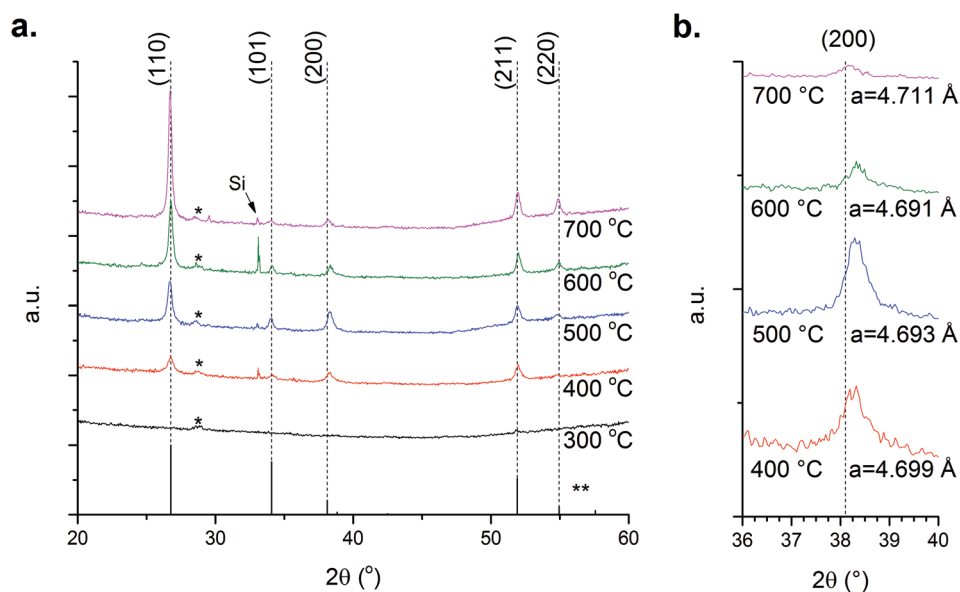

Fig. 1 XRD data for the SnO_2 films prepared at a fixed oxygen pressure (P_D) of 100 mTorr with temperature varied from 300–700 °C, (a) major peaks and phases identified on experimental data with stick reference pattern and dashed lines derived from ICDD 01-077-0452, the substrate peaks are clearly identified in addition to a small peak attributed to a minor SnO phase, (b) magnified analysis of the (200) diffraction peak and the calculated a-lattice parameter obtained for the films.

This journal is © The Royal Society of Chemistry 2016

J. Mater. Chem. C, 2016, 4, 758–765 | 759

two different crystallographic planes, extracted from Bragg's law ($n\lambda = 2d\sin\theta$):

$$\frac{1}{d^2} = \frac{h^2 + k^2}{a^2} + \frac{l^2}{c^2} \qquad (2)$$

The calculated a-lattice parameter shows a reduction as T increases from 400–600 °C but then increases when T is increased further, Fig. 1b. Such changes are indicative of intrinsic defects in the films. While Sn_i, oxygen interstitials (O_i) or doubly charged oxygen vacancies ($V_O^{\bullet\bullet}$) increase the size of the lattice V_O induces a reduction in lattice size.[11]

The measured film carrier concentrations are shown in Fig. 2a, the data show a clear reduction in the n-type carrier concentration by some three-orders of magnitude as T_D is increased. This suggests that the concentration of either Sn_i or V_O do not rise with T_D, as these are well-known n-type donor defects. The evolution of the optical band gap (E_g) and the Fermi level (E_F) as temperature is varied are shown in Fig. 2b. The E_g values above 400 °C are around 3.6 eV which is consistent with previous reports,[26] with the low value of 3.2 eV at 300 °C being attributed to band tailing effects present in amorphous films.[27] Similarly the increase in E_F as T_D is increased from 300 to 400 °C is also attributed to the band tailing effects, Fig. 2b. The E_F position is a product of electron chemical potential and surface dipole.[28] While the surface dipole is affected by the surface roughness[29–31] and the exposed crystal surface[32] we assume that these remain constant over the range of T_D investigated and that any contribution from surface dipole is negligible compared with the electron chemical potential which is directly influenced by the phase and structure of the materials, its stoichiometry and the presence of impurities and/or intrinsic/extrinsic defects.[33] More precisely,

the presence of either intrinsic or extrinsic defects is known to directly influence the position of the E_F[28,34,35] that can form additional occupied or unoccupied states within the E_g altering the carrier concentration and shifting the E_F within the band gap. In Fig. 3 the energy levels of several crystalline defects in the SnO_2 system are shown. This diagram gathers the defect transition energy levels, $\varepsilon(q/q')$ where q and q' are two charge states of the defect, extracted from literature calculations. In most models used in such calculations, $i.e.$ local-density approximation (LDA)[9] or the hybrid density functional theory (DFT),[36] the value of the band gap is underestimated and the
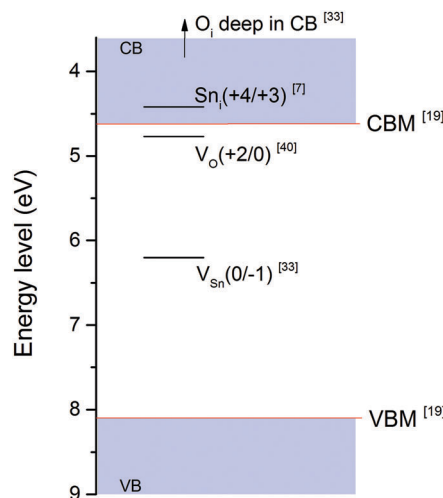

Fig. 3 Schematic representation of defect transition levels in SnO_2 in the form $D(q/q')$ where D is the defect, q the charge of the defect below the transition level and q' the charge above it (values extracted from ref. 7, 33 and 40. Valence band (VB) and conduction band (CB) represented in blue blocks. The valence band maximum (VBM) and the conduction band minimum (CBM) are represented by a red line (values from ref. 22).
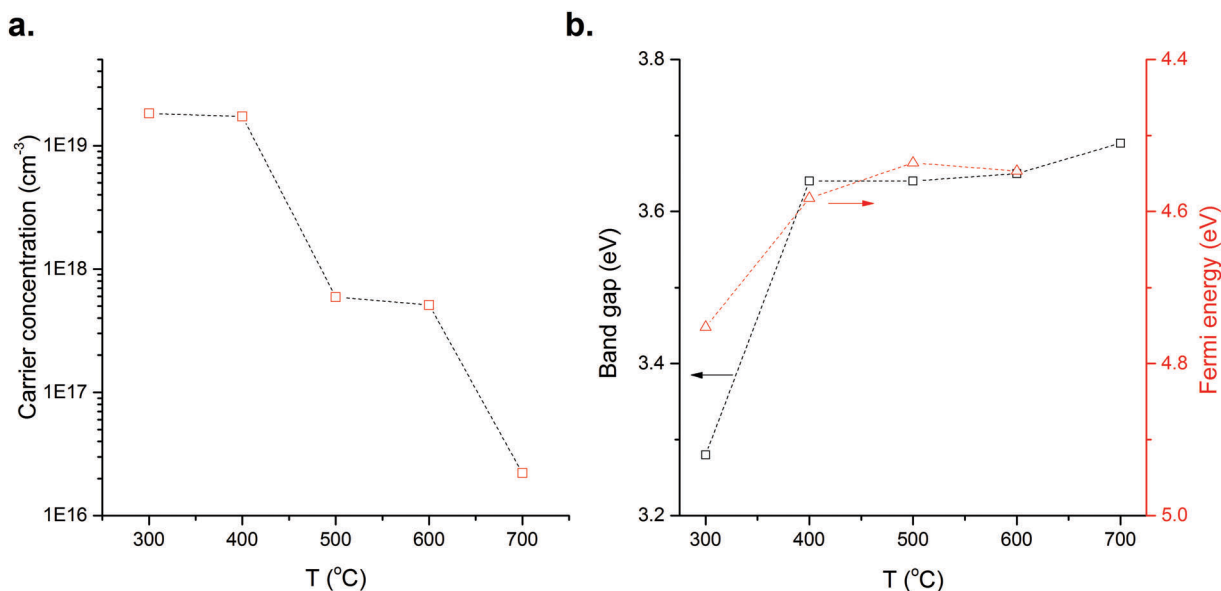

Fig. 2 Measured electrical and optical properties of the films deposited over the temperature range 300–700 °C, (a) carrier (electron) concentrations measured by AC Hall effect, (b) optical band gap calculated from Tauc analysis of UV-Vis data and measured Fermi levels.

760 | *J. Mater. Chem. C*, 2016, **4**, 758–765

This journal is © The Royal Society of Chemistry 2016

energy level of these defects may vary. Therefore the defects energies represented in Fig. 3 are an approximation of where such levels lie.

The charge of the defect is defined by the position of the E_F and the transition energy level of the defect $\varepsilon(q/q')$. V_O has a donor level 0.115 eV below the conduction band minima (CBM) for $\varepsilon_{V_O}(+2/0)$[9] and ionisation will only occur if the E_F lies below this level, otherwise the defect remains neutral. If we consider the CBM to be around 4.6 eV[22] the energy of $\varepsilon_{V_O}(+2/0)$ will be $\sim$4.7 eV. Measurements of E_F, Fig. 2b, show that at T_D above 400 °C values lie above 4.6 eV *i.e.* above the CB minima, thus the V_O present are likely to be in neutral state hence their contribution to change in electrical properties would be negligible and another defect must be responsible for the observed reduction in carrier concentration as T_D increases. More likely is a decrease in Sn_i which would explain both the reduction in a-lattice parameter and the fall in carrier concentration observed between 300 and 600 °C. The increase of the a-lattice parameter at 700 °C may be due to a reduction in V_O which, based on the E_f position, should be in a neutral charge state consequently inducing a compression of the lattice.[11] Other defects *i.e.* O_i or tin vacancies (V_{Sn}) may be present however the high substrate temperature may provide sufficient energy for Sn species in the plume to react with O and bring the system closer to stoichiometry. The presence of V_{Sn} in SnO2 thin films has been previously discussed,[37–39] however there presence in large concentrations has been ruled out owing to their high formation energy.[37]

Under the range of T_D investigated the presence of either tin or oxygen antisites are ruled out owing to their high formation energies.[36] Ke *et al.* studied the effect of annealing temperature in pure oxygen[40] where they observed an oxidation of the films above 500 °C leading to a decrease of V_O. It should be noted that the growth environment in our study differs from that

reported by Ke *et al.* hence we suggest a qualitative rather than quantitative comparison.

Therefore it may be logical to attribute the observed reduction in carrier concentration to a reduction of Sn_i and V_O through oxidation *i.e.* as T_D increases Sn has enough energy to fully react with molecular oxygen, leading to the formation of films closer to stoichiometry which is consistent with previous reports.[37] The temperature dependent variation in E_F, lattice constant and electrical properties are associated directly with a reduction in n-type defect concentration.

Influence of background oxygen pressure (P_D)

Films deposited at 700 °C had the lowest measured carrier concentrations, 2×10^{16} cm^{-3}, which would appear to be the optimum T_D for minimising donor defects. However owing to technical issues relating to sample mounting and subsequent analysis for variation of P_D a fixed T_D of 600 °C was chosen. Although 700 °C may appear to be the optimum T_D for reducing n-type defects, considerations regarding the sample mounting and thermal degradation of ITO (thus directly impacting E_F measurements) must be made. We suggest that 600 °C is adequate to balance processing restrictions with optimum characteristics, thus studies to elucidate the impact of P_D were carried out at this temperature.

The XRD data show that SnO2, Fig. 4a, films still exhibit a preferential (110) orientation, however we observe a shift in the preferred orientation as P_D varies. At low P_D the growth is dominated by the (101) orientation. This peak almost disappears when P_D increases to 50 mTorr with a change to (110) oriented films. Further increases in P_D result in the appearance of (101) and (211) preferred orientations. This is quantified through analysis of the TC, summarised in Table S2.† The behaviour observed at low P_D, *i.e.* 5 mTorr, may be attributed to the highly energetic ablated
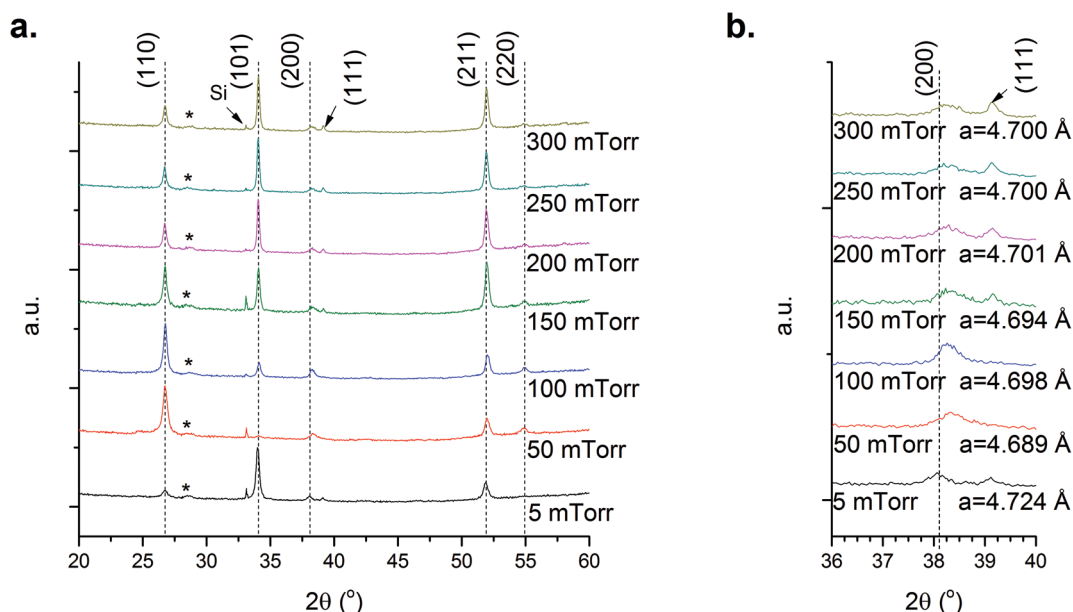

Fig. 4 XRD data for the SnO2 films prepared at a fixed temperature of 600 °C with the oxygen pressure varied from 5–300 mTorr, symbols and dashed lines as Fig. 1, (a) SnO2, and (b) magnified analysis of the (200) diffraction peak and the calculated a-lattice parameter obtained for the films.

This journal is © The Royal Society of Chemistry 2016

J. Mater. Chem. C, 2016, **4**, 758–765 | **761**

species in the plume as a result of reduced interaction with molecular oxygen, promoting growth not supported under other conditions.[22] Introduction of molecular oxygen into the chamber, i.e. for 5–50 mTorr, lead to a corresponding shift in a-lattice parameter, Fig. 4b, which may also be attributed to a decrease in the concentration of Sn_i defects. This is supported by Kılıç and Zunger who showed the formation energy of Sn_i decreases in oxygen-deficient environments.[9] Consequently, the combined Sn-rich/O-poor environment would favour the formation of Sn_i over V_O. Above 50 mTorr, the lattice parameter shows a subtle gradual increase until 200 mTorr. To understand the impact of structural variation and its origin we probe the extracted carrier concentrations in Fig. 5a, where it is shown that increasing P_D over the range studied results in a three-orders of magnitude reduction in carrier concentration. This may be explained through a reduction in V_O or the presence of O_i or V_{Sn} to compensate the n-type defects. The formation energies of O_i and V_{Sn} decrease under oxygen-rich conditions and the presence of these defects would contribute to the subtle increase in a-lattice parameter and with the reduction in carrier concentration. As with T_D variation we consider that such defects will be present in small quantities owing to their high formation energy.[36] It remains more plausible that as P_D is increased, the system again approaches to stoichiometry by incorporating more oxygen, this is supported by Scanlon and Watson[36] who demonstrated that the formation energy of V_O and Sn_i increases when the environment becomes oxygen-rich.

The E_g values for all P_D values are around 3.6–3.7 eV, Fig. 5b, with no systematic variation observed with the change in processing conditions. However, there is a sharp decrease in the E_F values above 150 mTorr. This shift towards the centre of the E_g can be interpreted as support for the structure moving towards stoichiometry where in the stoichiometric state the E_F of a metal oxide should lie halfway between the top of the VB and the bottom of the CB.[34,35] Globally the increase in P_D

results in a decrease in the charge carrier concentration attributed to a reduction in the concentration of Sn_i and V_O. Thus, the SnO_2 films approach stoichiometry by limiting the amount of donor type defects. Identifying the experimental conditions at which this occurs is essential for the development of p-type SnO_2 i.e. it is necessary to eliminate the formation of n-type defects to avoid charge compensation when p-type defects are introduced. Based on the results presented we consider that a T_D of 600 °C and a P_D of 250 mTorr of oxygen are sufficient to significantly reduce the concentration of Sn_i and V_O.

Influence of target surface composition

For PLD, the T_D and the P_D constitute perhaps the two most important and widely investigated parameters to vary during growth. What is often overlooked is the composition of the target before, during and after deposition – whilst the initial cation concentrations can be controlled during target preparation this value may change during laser exposure. This was exemplified by Claeyssens et al.[41] who studied this in the ZnO system. Specifically, the authors observed a Zn enrichment on ablated targets due to backscattering from the plasma plume and subsequent condensation on the target surface. The least volatile component condenses first i.e. Zn, leading to the Zn rich surface. This observation partly explains why non-stoichiometric films are deposited when a target is used for extended periods. In the data presented above we have eliminated such effects by polishing the target between successive depositions. However, to fully investigate the influence of target composition changes in the SnO_2 system we compare the experimental data shown previously with data obtained using an unpolished target that was subjected to >100 000 pulses. In particular, we do so by fixing T_D and varying P_D over the range 5–300 mTorr.
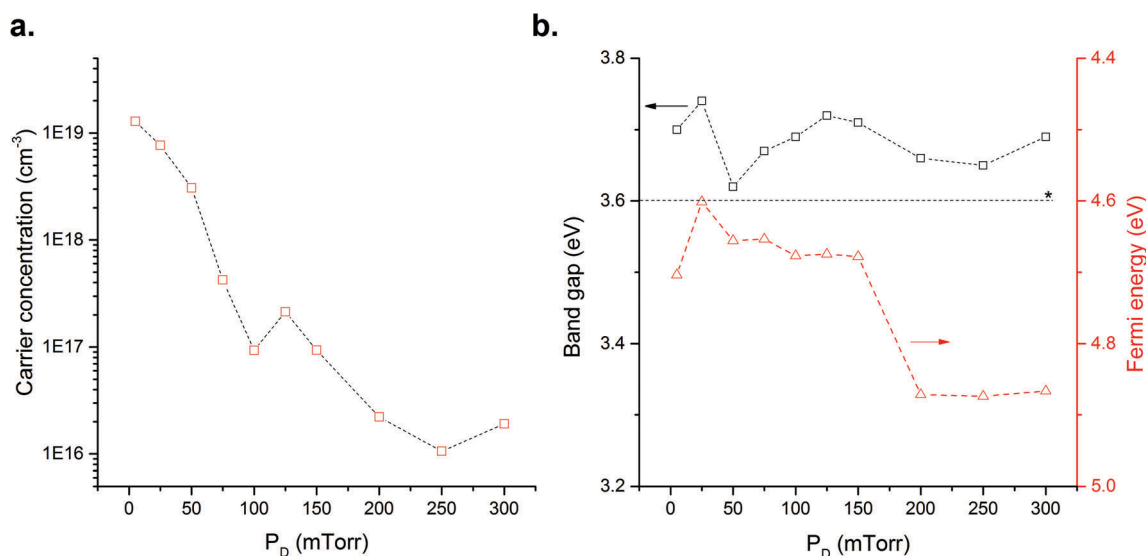

Fig. 5 Measured electrical and optical properties of the films deposited over the background oxygen pressure range 5–300 mTorr, (a) carrier (electron) concentrations measured by AC Hall effect, (b) optical band gap calculated from Tauc analysis of UV-Vis data and measured Fermi level. *Band gap value from Batzill et al.[26]
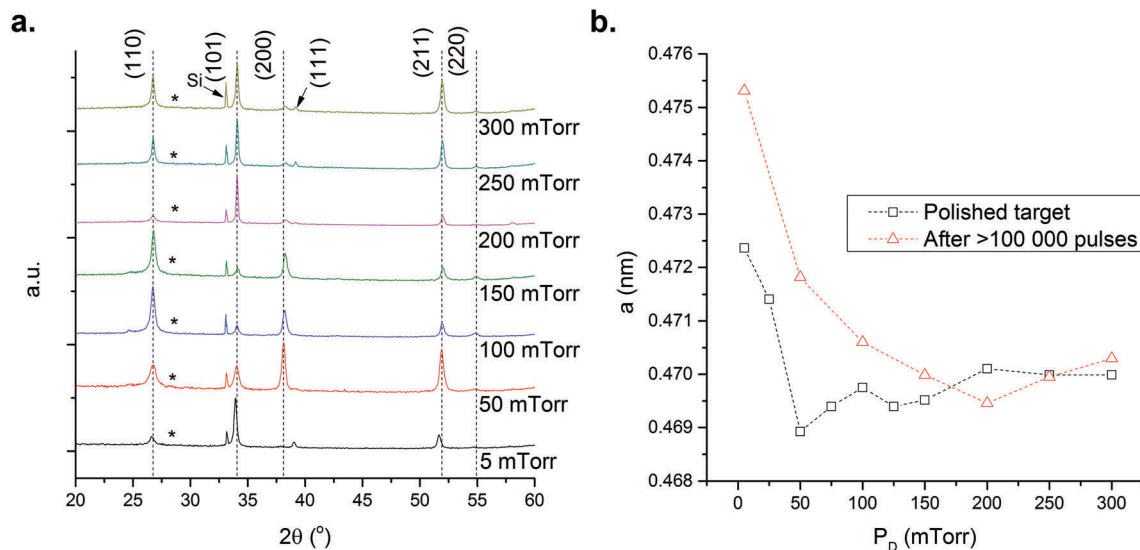
Fig. 6 XRD data for the SnO$_2$ films prepared using a SnO$_2$ target exposed to >100 000 laser pulses at a fixed temperature of 600 °C with the oxygen pressure varied from 5–300 mTorr, symbols and dashed lines as Fig. 1.

Fig. 6a shows the XRD data obtained during the variation of P_D using an exposed target. Similar behaviour to that observed previously for polished targets is seen at P_D = 5 mTorr, with a strong preferred (101) orientation and a noticeable increase in the relative intensity of the (211) diffraction peak. Increasing P_D from 50–150 mTorr results in the appearance of a strong (200) peak and a reduction in the (211) intensity. At 200 mTorr the (211) peak dominates the diffraction data and at higher P_D values *i.e.* >250 mTorr the data for polished and unpolished targets are comparable. Changes in the XRD data with increased P_D are attributed to a reduction in V$_O$. However, when comparing the *a*-lattice parameters for films prepared from the exposed and polished targets it is apparent that at P_D < 200 mTorr the *a*-lattice parameter obtained from the polished target is smaller, Fig. 6b.

This is exemplified by examining the carrier concentrations and E_F of the films prepared, Fig. 7a. The carrier concentrations for the unpolished films are significantly higher at all P_D values than those prepared from a polished target. At low P_D, *i.e.* below 100 mTorr, there is little fluctuation as P_D is increased owing to the high Sn$_i$ concentration that cannot be compensated for by the increased oxygen content of the chamber. Above 100 mTorr the carrier concentration falls by more than one order of magnitude as the Sn$_i$ defects begin to be compensated by V$_O$ filling. However, we suggest that a significant concentration of Sn$_i$ persists which accounts for the increased carrier concentrations and the larger measured *a*-lattice constant. Thus the combination of structural, XRD, and electrical characteristics give a direct insight into the defect species dominating the
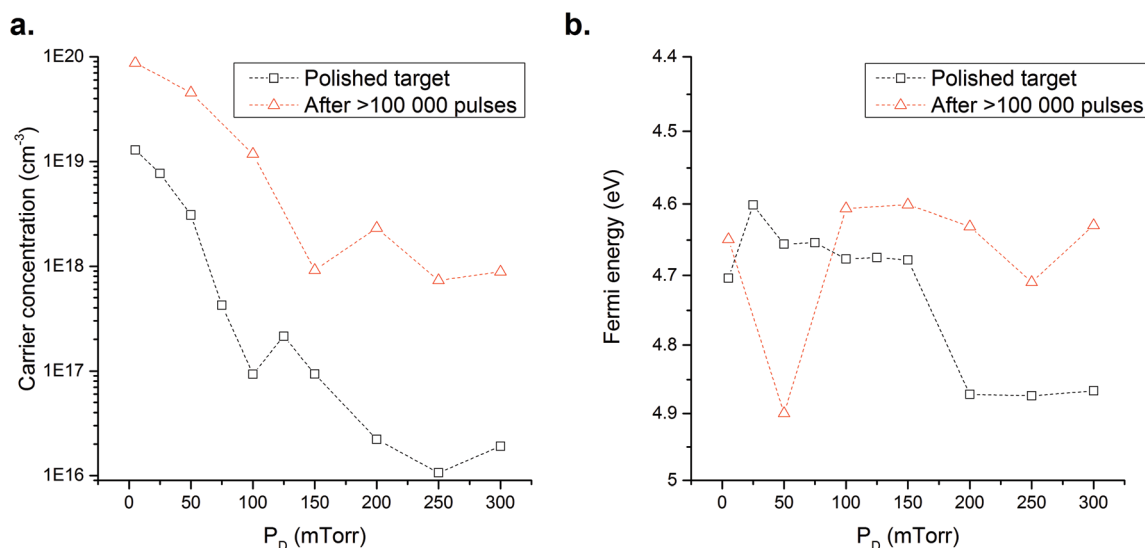

Fig. 7 Data of SnO$_2$ films deposited at 600 °C and under 5–300 mTorr comparing the films with a clean target and with the target exposed to >100 000 laser pulses showing (a) carrier concentration, and (b) Fermi level (E_f) evolution.

films. Similar to films prepared from polished targets those deposited from the exposed target get closer to stoichiometry as P_D is increased, but even at the highest P_D studied (300 mTorr) the carrier concentration of these films are some two-orders of magnitude greater than those prepared from polished targets. This highlights the issue of Sn recondensation on the target surface, the creation of an Sn rich growth environment and the resultant impact on measured electrical properties. Concerning the defects present in the films, we conclude that two effects are being observed in parallel with the unpolished target (i) an increase in Sn_i owing to Sn enrichment of the target surface, and (ii) a reduction in V_O attributed to the increased amounts of oxygen.

Analysis of the E_F position for films prepared with exposed targets shows some considerable variations, particularly at $P_D < 100$ mTorr where the value at 50 mTorr falls to 4.9 eV compared with 4.65–4.6 eV at 5 and 100 mTorr. Whilst the 50 mTorr value may appear to be an outlier, it has been reconfirmed several times by repeat measurements. Such a shift could be characteristic of a change in defect nature within the lattice. While most of the defect energy levels have been estimated theoretically, Fig. 4, the V_O energy level has been extracted experimentally by Samson and Fonstad[42] to lie just below the CB minima (150 meV below in the case of the second ionized level of V_O) with the CB edge established at around 4.6 eV.[22] Here we suggest that the extremely high carrier concentrations and the variation in E_F could be attributed to a shift of the dominant defect from Sn_i (energy above the CB[9]) toward V_O. Whist this may not be intuitive we believe the increase in oxygen content in the chamber raises the formation energy of Sn_i above that of V_O. This matter has been widely discussed by Kılıç and Zunger,[9] Singh et al.[11] and Godinho et al.[8] where either Sn_i or V_O form preferentially in SnO_2. However the formation of a preferred defect is subject to its environment. Furthermore, as the carrier concentration of the exposed target films is maintained above 10^{19} cm^{-3}, Fig. 7a, the presence of a defect other than Sn_i is indicated (e.g. V_O) in order to ensure the formation of n-type charge carriers. Greiner et al.[28] suggest a decrease of the work function as the oxidation state decreases. This would translate to the E_F moving towards the CB as more V_O are formed. However we believe this effect is limited by the presence of other defects such as Sn_i whose formation energy lies above the CB minima.

Conclusions

We report a detailed investigation of the structural and electronic properties of SnO_2 films grown by pulsed laser deposition (PLD). By independently studying the growth temperature (T_D) and growth chamber oxygen gas pressure (P_D) we have identified growth conditions that allow significant control over intrinsic defect levels in our films. Considering T_D, we show significant changes over the temperature range 300–700 °C attributed to a marked change in Sn_i and V_O concentrations. At low temperatures, <500 °C, Sn_i and V_O dominate the defect chemistry resulting in

films with high charge carrier concentrations $>2 \times 10^{19}$ cm^{-3} reducing to 2×10^{16} cm^{-3} at 700 °C – associated with thermal oxidation not possible at lower temperatures.

For P_D variation we again observe a change in the structure associated with defect formation. In this case, deposition below 50 mTorr results in large concentration Sn_i rather than V_O. Here the films show a near three-orders of magnitude reduction in carrier concentration when P_D is increased from 50–300 mTorr associated with the removal of these n-type donor defects and a shift towards more stoichiometric SnO_2. In support of this theory the measured Fermi level (E_F) shift from near the conduction band towards the middle of the band-gap (E_g) at $P_D > 150$ mTorr which is consistent with a system moving towards stoichiometry.

In the final section we consider the importance of the PLD target surface, which by exposing to >100 000 laser pulses becomes metal rich. When T_D is fixed and P_D varied over the same range as previously studied carrier concentrations approaching 1×10^{20} electrons per cm^{-3} (50 mTorr) are measured. The enrichment of Sn on the target surface significantly increases the concentration of Sn_i in the films – supported by the XRD data. The large concentration of Sn_i cannot in this case be compensated for by increasing P_D, although the carrier concentration reduces with increasing P_D, the E_F position remains close to the conduction band indicating that Sn_i defects are present in large concentrations.

In conclusion we show the relationship between the main processing parameters, namely T_D, P_D and target surface composition on the measured microstructural and electrical properties of SnO_2 films. We demonstrate the ability to accurately control charge carrier mobility and charge carrier concentration enabled by understanding and controlling intrinsic defect formation as a function of deposition conditions.

Methods and materials

Thin-film deposition

The SnO_2 target was sourced commercially (Mateck, purity = 99.99%, $\delta > 95\%$). Films were deposited using a KrF excimer laser ($\lambda = 248$ nm, pulse duration = 25 ns, frequency = 8 Hz) at a base pressure of 10^{-5} Torr with the oxygen background gas pressure controlled between 5 and 300 mTorr. The incident laser fluence was set at 2.2 J cm^{-2} for all depositions. The distance between target and substrate was fixed at 50 mm. Films were deposited on quartz (UQG optics, PFS-1010), silicon (100) (Crystal Gmbh) and ITO coated glass (PsiOTec Ltd, 15 Ohm per sqr) at temperatures between 300–700 °C. Prior to growth, all substrates were cleaned by sequential ultra sonication in acetone, ethanol and isopropanol and immediately prior to deposition by UV-ozone exposure.

Film characterisation

The structure and phase of the films were assessed via XRD using a PANalytical X'Pert system (Cu Kα, $\lambda = 1.54$ Å) between 20–60° (2θ). Film thickness measurements were obtained using a Dektak surface profilometer; the measured film thicknesses for T_D variation were in the range 180 ± 6 nm and for P_D variation 298 ± 31 nm. AC

764 | J. Mater. Chem. C, 2016, 4, 758–765

This journal is © The Royal Society of Chemistry 2016

Hall measurements were performed on the films deposited on quartz using a Lakeshore 8400 system with current between 10 nA and 50 mA, and with AC magnetic field of 1.19 T. The optical transmittance was measured on quartz using a Bentham 605 custom optical bench between 250–800 nm. The optical band gaps were calculated using the Tauc model for direct band gap semiconductor. The Fermi levels were measured *via* the Kelvin Probe technique, specifically using a SKP5050 from KP technology. The analysis was performed in air on the films deposited on ITO to avoid local charging effects.

Acknowledgements

References

1 R. E. Presley, C. L. Munsee, C.-H. Park, D. Hong, J. F. Wager and D. A. Keszler, *J. Phys. D: Appl. Phys.*, 2004, **37**, 2810–2813.

2 G. J. Exarhos and X.-D. Zhou, *Thin Solid Films*, 2007, **515**, 7025–7052.

3 H. Liu, V. Avrutin, N. Izyumskaya, Ü. Özgür and H. Morkoç, *Superlattices Microstruct.*, 2010, **48**, 458–484.

4 S. Sheng, G. Fang, C. Li, S. Xu and X. Zhao, *Phys. Status Solidi A*, 2006, **203**, 1891–1900.

5 J. B. Franklin, J. B. Gilchrist, J. M. Downing, K. A. Roy and M. A. McLachlan, *J. Mater. Chem. C*, 2014, 84–89.

6 J. B. Franklin, L. R. Fleet, C. H. Burgess and M. A. McLachlan, *Thin Solid Films*, 2014, **570**(Part), 129–133.

7 T. Yang, X. Qin, H. Wang, Q. Jia, R. Yu, B. Wang, J. Wang, K. Ibrahim, X. Jiang and Q. He, *Thin Solid Films*, 2010, **518**, 5542–5545.

8 K. G. Godinho, A. Walsh and G. W. Watson, *J. Phys. Chem. C*, 2009, **113**, 439–448.

9 Ç. Kılıç and A. Zunger, *Phys. Rev. Lett.*, 2002, **88**, 095501.

10 C. Kılıç and A. Zunger, *Appl. Phys. Lett.*, 2002, **81**, 73.

11 A. K. Singh, A. Janotti, M. Scheffler and C. G. Van de Walle, *Phys. Rev. Lett.*, 2008, **101**, 055502.

12 C. G. Van de Walle, *Phys. Rev. Lett.*, 2000, **85**, 1012–1015.

13 D. M. Hofmann, A. Hofstaetter, F. Leiter, H. Zhou, F. Henecker, B. K. Meyer, S. B. Orlinskii, J. Schmidt and P. G. Baranov, *Phys. Rev. Lett.*, 2002, **88**, 045504.

14 M.-M. Bagheri-Mohagheghi and M. Shokooh-Saremi, *J. Phys. D: Appl. Phys.*, 2004, **37**, 1248–1253.

15 S. F. Ahmed, S. Khan, P. K. Ghosh, M. K. Mitra and K. K. Chattopadhyay, *J. Sol-Gel Sci. Technol.*, 2006, **39**, 241–247.

16 F. Finanda, H. C. Ma and H. Y. Lee, *Ceram. Prog. Res.*, 2012, **13**, 181–185.

17 Y. Huang, Z. Ji and C. Chen, *Appl. Surf. Sci.*, 2007, **253**, 4819–4822.

18 J. M. Ni, X. J. Zhao and J. Zhao, *J. Inorg. Organomet. Polym. Mater.*, 2011, **22**, 21–26.

19 B. Falabretti and J. Robertson, *J. Appl. Phys.*, 2007, **102**, 123703.

20 E. Elangovan and K. Ramamurthi, *Appl. Surf. Sci.*, 2005, **249**, 183–196.

21 J. B. Franklin, B. Zou, P. Petrov, D. W. McComb, M. P. Ryan and M. A. McLachlan, *J. Mater. Chem.*, 2011, **21**, 8178–8182.

22 R. Easton, *Pulsed Laser Deposition of thin film: Applications-Led growth of functional materials*, John Wiley & sons, 2007.

23 C. R. Foschini, L. Perazolli and J. A. Varela, *J. Mater. Sci.*, 2004, **39**, 5825–5830.

24 Z. W. Chen, C. M. L. Wu, C. H. Shek, J. K. L. Lai, Z. Jiao and M. H. Wu, *Crit. Rev. Solid State Mater. Sci.*, 2008, **33**, 197–209.

25 C. S. Barrett and T. B. Massalski, *Structure of Metals: Crystallographic Methods, Principles and Data*, 1980.

26 M. Batzill and U. Diebold, *Prog. Surf. Sci.*, 2005, **79**, 47–154.

27 J. Lee, *Thin Solid Films*, 2008, **516**, 1386–1390.

28 M. T. Greiner and Z.-H. Lu, *NPG Asia Mater.*, 2013, **5**, e55.

29 W. Li and D. Y. Li, *J. Chem. Phys.*, 2005, **122**, 064708.

30 R. Smoluchowski, *Phys. Rev.*, 1941, **60**, 661–674.

31 Y.-J. Lin, I. D. Baikie, W.-Y. Chou, S.-T. Lin, H.-C. Chang, Y.-M. Chen and W.-F. Liu, *J. Vac. Sci. Technol., A*, 2005, **23**, 1305.

32 R. W. Strayer, W. Mackie, L. W. Swanson and S. Admin, *Surf. Sci.*, 1973, **34**, 225–248.

33 M. T. Greiner, L. Chai, M. G. Helander, W.-M. Tang and Z.-H. Lu, *Adv. Funct. Mater.*, 2012, **22**, 4557–4568.

34 M. Ohring, *The Materials Science of Thin Films*, 1992.

35 J. S. Blakemore, *Solid State Physics*, Cambridge University Press, 2nd edn, 1985.

36 D. O. Scanlon and G. W. Watson, *J. Mater. Chem.*, 2012, **22**, 25236.

37 Z. Chen, D. Pan, Z. Li, Z. Jiao, M. Wu, C.-H. Shek, C. M. L. Wu and J. K. L. Lai, *Chem. Rev.*, 2014, **114**, 7442–7486.

38 G. Rahman, V. M. García-Suárez and S. C. Hong, *Phys. Rev. B: Condens. Matter*, 2008, **78**, 184404.

39 S. B. Ogale, R. J. Choudhary, J. P. Buban, S. E. Lofland, S. R. Shinde, S. N. Kale, V. N. Kulkarni, J. Higgins, C. Lanci, J. R. Simpson, N. D. Browning, S. Das Sarma, H. D. Drew, R. L. Greene and T. Venkatesan, *Phys. Rev. Lett.*, 2003, **91**, 077205.

40 C. Ke, W. Zhu, J. S. Pan and Z. Yang, *Curr. Appl. Phys.*, 2011, **11**, S306–S309.

41 F. Claeyssens, A. Cheesman, S. J. Henley and M. N. R. Ashfold, *J. Appl. Phys.*, 2002, **92**, 6886.

42 S. Samson and C. G. Fonstad, *J. Appl. Phys.*, 1973, **44**, 4618.